PRELIMINARY OBSERVATIONS ON NANOPRECIPITATES IN IRON METEORITES. Laurence A.J. Garvie[1,2], [1]Center for Meteorite Studies, [2]School of Earth and Space Exploration, Arizona State University, 781 East Terrace Rd., Tempe, AZ 85287-6004 (lgarvie@asu.edu).

Introduction: Trace elements in iron meteorites are used to model crystallization processes that occurred within asteroidal cores and to help elucidate the formation and thermal history of metal during nebular and planetary differentiation processes. While trace elements are determined by a number of analytical techniques such as SIMS and laser ablation ICPMS, these methods provide little data on the trace-element hosts. Studies of steels and alloys reveal that minor and trace elements often concentrate in nanoparticles, and there has been extensive study of their formation. Their chemistry, morphology, and distribution provide key information on a samples' thermal history. Further, the role of trace elements in alloy formation, solidification, and physical properties is well documented. In contrast, there are virtually no studies of non-metal and platinum-group element (PGE)-rich nanoparticles in iron meteorites.

Polished sections of many iron meteorites reveal a Widmanstätten structure composed of several Fe-Ni phases, interspersed with non-metallic components, most commonly troilite FeS, schreibersite $(Fe,Ni)_3P$, cohenite $(Fe,Ni,Co)_3C$, and graphite [1-4]. A host of other precipitates occur, including carbides, nitrides, oxides, sulfides, and phosphates [1, 3, 5-10]. High-resolution imaging continues to reveal new precipitates, such as the recently described joegoldsteinite, $MnCr_2S_4$ [11]. A characteristic of most non-metallic precipitates described from irons is their large sizes, typically micron or larger. Yet, the preliminary studies described here, and those of steels and alloys, reveal an abundance of nanometer-sized particles [12-15]. In contrast with the steel industry where nanoparticles are a mature field of study (e.g., [12], there are few such studies for iron meteorites.

Although metal nanoparticles are known from high-spatial-resolution meteorite studies, e.g., [16, 17], observations of Fe-Ni-free nanoparticles in iron meteorites are sparse. Our goal is to reveal the nanoparticle structures, compositions, and distributions within metal of iron meteorites and stony irons and to characterize the trace-element hosts and its implications for meteorite history.

Materials and methods: Nanoparticles were searched for in the metal of seven iron meteorites and one pallasite: Odessa and Canyon Diablo (IAB-MG), Gressk (IIAB), Henbury (IIIAB), Gibeon (IVA), Butler and Deep Springs (ungrouped), and Brenham (PMG-an). Particle extraction involves etching the metal so that the insoluble particles protrude above the metal surface. A thin ~10-nm layer [13], of amorphous C (hereafter called the lift-off film) is then evaporated onto the metal; this film is gently scored into ~2-mm-squares. Samples are then re-immersed into the etchant. The lift-off film squares, with the attached precipitates, float off the metal surface and are captured on a 3-mm-diameter Ti or Al 100 mesh TEM grid. No Al and few Ti-bearing nanoparticles were found in the preliminary work, so possible stray x-ray peaks generated during EDX analysis in the TEM will not interfere with the particle analysis.

Ensuring that the nanoparticles are indigenous to the iron meteorites: Care was taken to clean the metal surfaces before etching and coating with C. Failure to clean the surfaces can result in the incorporation of foreign particles in the metal from the cutting, grinding, and polishing. In order to exclude foreign particles, surfaces were cleaned with physical and chemical methods. With physical cleaning, a lath-bit with a single-crystal of cubic BN was used to plane away ~100 mm of the cut and flat surface. This new clean surface was then etched with nital (nitric acid in methanol). After etching, the planed surface showed only minor distortion of the metal structure. For chemical cleaning, liquid Br was used: this liquid rapidly and simultaneously dissolves both the Ni-rich and poor metal leaving a shiny, flat, clean surface. This surface can then be further etched with nital. In summary, the nanoparticles described below were all extracted from uncontaminated metal and are indigenous to the sample.

Results: Abundant nanoparticles were found in all samples. These particles display a variety of compositions, shapes, sizes, and concentrations. Using TEM, EDS, and EELS eight new types of nanoparticles (sizes between 1 nm and 1 micron) were discovered: Pd-Zn and Pd-Sn binary alloys, PGE nuggets, Ge- and Ga- rich Ni phosphides, Cr-Mo nitrides, and Cr sulfides with PGEs, and a Ga-rich silicate. These nanoparticles are locally abundant and hosts for several siderophile and chalcophile trace elements. Samples were prepared using techniques I used in previous studies of nanoparticles in steels [13-15], which involves etching the metal, coating with C, removing the film with nital, and capture of the film on TEM grids. Precipitates that were left proud of the metal surface by the first nital etch are encased in the evaporated C, and then liberated from the metal by the second etch. The electron-dense precipitates are visible by TEM on the C film free of the encasing Fe-Ni (Fig. 1).

PGE-rich and binary Pd-Sn/Zn grains: Despite the low abundances of PGEs in iron meteorites, their concentration in nanoparticles allows them to be characterized by TEM. These nanoparticles display a range of sizes (1 to 500 nm) and compositions. Palladium is the most abundant PGE encountered; it is commonly with As, Sn, Sb, In, Zn, and Au. For example, Canyon Diablo contains < 20-nm Pd-Au (±As) particles. Butler contains the widest range of PGE particle types and also the most Ge-rich precipitates. Up to 10 at % Ge occurs in particles containing the following elements: Pd-Zn, Pd-Zn-Rh-Ru-Pt, Fe-Ni-P, Ni-Sn, and Fe-Ni-Pt-Ru. Odessa contains small rounded Pd-Sn particles (Fig. 1). The high Ge content of the Butler precipitates reflects the

anomalously high content of this element, with up to 2000 ppm [18-20].

Ge-rich phosphides: A new nanoparticle was discovered in Gibeon with a composition close to $Ni_{12}P_5$. Butler contains abundant, rounded, Ge-rich Fe-Ni-P particles (<100-nm across), whose location parallels the coarse kamacite spindles. Brenham contains abundant, small Ni-P and larger rounded Fe-Ni-P particles in the swathing kamacite. Ge-bearing Fe-Ni-P particles occur in Odessa.

Mo-rich nitrides: Chromium nitride and sulfide are locally common (typically < 300 nm grains). Their presence is consistent with the incompatibility of Cr in low-S, Fe-Ni melts [21]. The most common accessory element is Mo, with up to 50 at% replacement of Mo for Cr. The composition of the Mo- and Fe-free grains is close to $CrN_{1.1\pm0.1}$ (carlsbergite), as determined by EELS. Chromium sulfide (±Fe, Cu, Pd, Ru, As) occurs in Deep Springs, Brenham, and Gressk.

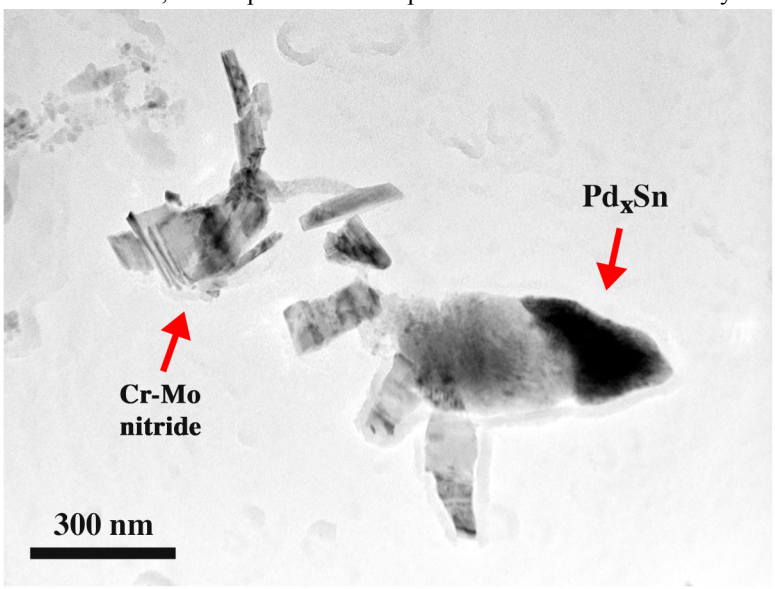

Figure 1. Bright-field TEM image of a cluster of nanoparticles from Odessa supported on an amorphous C film. The Pd-Sn particle (dark) is attached to a Cr-Mo nitride particle.

Ga-rich silicate: Stubby laths, to 300 nm, of an Fe-Ga-P silicate are locally abundant in several of the Odessa samples. Discovery of Ga with a silicate may explain the abundance trends for this element seen in some irons, which cannot be modeled for any S concentration: the conclusion is that the depletions my reflect decreased siderophilic behavior in a relatively oxidized body and partitioning of the Ga into the silicate portion of the parent body [22].

Composite nanoparticles: These particles were found in Canyon Diablo and Odessa (Fig. 1). Some Mo-Cr nitrides in Odessa have adhering caps of Pd-Sn, and in Canyon Diablo many of the large Cr-Mo nitrides have adhering Fe-Ni-P particles. Composite nanoparticles can provide information on the precipitation sequence [13,14].

Nanoparticle abundances and distribution: The abundances of nanoparticles vary widely. For example, in Butler there were ~20 binary Pd-Zn particles, 50 to 100 nm in size, on one 3-mm TEM grid. The ease of "seeing" these particles with TEM is possible because of their high electron density relative to the low Z support film. Another Butler grid contained fewer PGE-rich particles but had a higher abundance of Ge-rich Fe-Ni phosphides. Particle types also varied with respect to the metal structure. For example, in Brenham, PGE and Cr-S particles occur in the plessite, whereas Fe-Ni-P and Ni-P particles are abundant in the kamacite.

Conclusions: It is important to reveal the locations and sites of trace elements in iron meteorites, as these elements provide information on a samples thermal history and can be used to model crystallization processes. In addition, these elements are the basis for our current iron meteorite classification system. The preliminary results show an abundance of previously undescribed nanoparticles in iron meteorites; these particles are the hosts for a range of geochemically important trace elements, such as Pd, Mo, and N.

Acknowledgement: Support for this research was provided by the NASA Emerging Worlds (EW) program through grants NNX15AH62G and NNH16ZDA001N.

References: [1] Buchwald, V.F., *Handbook of Iron Meteorites*. Vol. 1 to 3. 1975, Berkeley and Los Angeles, California, USA: Arizona State University and University of California Press. [2] Goldstein, J.I. and H.J. Axon, Naturwissenschaften, 1973, **60,** 313-321. [3] Rubin, A.E., *MAPS*, 1997, **32,** 231-247. [4] Yang, J. and J.I. Goldstein, *MAPS*, 2005, **40,** 239-253. [5] Axon, H.J., et al., Min Mag, 1981, **44,** 107-109. [6] Bunch, T.E. and L.H. Fuchs, Am Min, 1969, **54,** 1509-1518. [7] Mittlefehldt, D.W., et al., *Planetary Materials*, J.J. Papike, Editor. 1998, Mineralogical Soc Amer: Chantilly. p. D1-D195. [8] Nielsen, R.L. and V.F. Buchwald, *LPSC* 1981. **12B**, 1343-1348. [9] Scott, E.R.D., Nature, 1971, **229,** 61-62. [10] Skála, R. and I. Císařová, Phys Chem Miner, 2005, **31,** 721-732. [11] Isa, J., C. Ma, and A.E. Rubin, Am Min, 2016, **101,** 1217-1221. [12] Baker, T.N. *Microalloyed steels.* Ironmaking and Steelmaking, 2016, 1-44. [13] Craven, A.J., et al., Acta Materialia, 2000, **48**, 3857-3868. [14] Craven, A.J., et al., Acta Materialia, 2000, **48,** 3869-3878. [15] Kejian, H., et al., Electron Microscopy 1994, Proceedings of the XIIIth International Congress on Electron Microscopy, 1994. **1**: p. 665-666. [16] Zhang, J., et al., Surface Science, 1992, **266,** 433-440. [17] Zhang, J., D.B. Williams, and J.I. Goldstein, Geochim Cosmochim Acta, 1993, **57,** 3725-3735. [18] Goldstein, J.I., 1966, **153,** 975-976. [19] Goldstein, J.I., J Geophys Res, 1967, **72,** 4689-4696. [20] Wasson, J.T., Science, 1966, **153,** 976-978. [21] Bild, R.W. and M.J. Drake, *LPSC*, 1978, **9,** 1407-1421. [22] McCoy, T.J., et al., Geochim Cosmochim Acta, 2011, **75,** 6821-6843.